Heterogeneous Catalysis

DOI: 10.1002/anie.200905181

Platinum Sintering on H-ZSM-5 Followed by Chemometrics of CO Adsorption and 2D Pressure-Jump IR Spectroscopy of Adsorbed Species**

*Mickaël Rivallan, Etienne Seguin, Sébastien Thomas, Muriel Lepage, Nobuyuki Takagi, Hirohito Hirata, and Frédéric Thibault-Starzyk**

Platinum catalysts are important materials for green chemistry and car exhaust treatment.[1–3] Under working conditions, Pt nanoparticles, reported as the catalytic centers of the reactions, are unfortunately subject to deactivation due to migration and further Pt agglomeration. From this so-called sintering mechanism, many important points remain a matter of debate, especially since conventional optical characterization methods do not provide crucial parameters such as Pt location.[4,5] For example, CO chemisorption sheds light on the metal dispersion and its combination with infrared (IR) spectroscopy can improve the accuracy of the results.[6–11] This technique is, however, only fairly sensitive because it only yields an average value of dispersion and only one type of Pt nanoparticle is generally considered, whereas transmission electron microscopy (TEM) often reveals the presence of various Pt nanoparticles, differing in size and shape,[12,13] depending on the preparation, support, and thermal treatment.[6,14–28] None of these techniques gives clear information on where the Pt nanoparticles are positioned on the zeolite support, although they constitute the core of the catalytic reactions. The location of the Pt nanoparticles on the ZSM-5 support could be tuned (mesoporosity, microporosity, outer surface) and could result in distribution in different classes of Pt nanoparticles (after thermal treatments, catalytic processes). This control of the location of the catalytic center is also likely to affect strongly the efficiency of the catalyst, first because it may influence the accessibility of the Pt metal to the reactant gas, and second because it could also limit the agglomeration when Pt is confined into the pores.

In order to gain information on the sintering mechanisms of Pt nanoparticles supported onto ZSM-5 zeolites (2.0 wt.% Pt), we report herein the combination of chemometric analysis of CO chemisorption with two-dimensional pressure-jump IR spectroscopy of adsorbed species (2D PJAS-IR)[29,30] to shed light on the distribution and location of the metal particle.

Three different methods were used for dispersing Pt on the zeolite (Table 1). TEM of the samples prepared by zeolite wet impregnation (WI) (Figure 1) shows two classes of Pt nanoparticles differing in size. The particles we detected have an average size larger than 2.5 nm and are not expected to be located in the micropores but rather in the mesopores and on the outer surface. For samples prepared from colloidal impregnation (CI), no Pt nanoparticles are expected inside the pores of the ZSM-5 support (the colloid is too large), whereas for samples prepared after ion exchange (IE), the larger agglomerates are long, thin cylindrical particles probably shaped by the mesoporosity.[31]

CO chemisorption[31] (Table 1) confirms the TEM observations that the Pt particles greatly sinter with around three times lower dispersion after air treatment, whereas the surface and pores of the zeolite matrix (Table 1) remain stable (and encapsulation of Pt into plugged pores can be neglected). Chemometric analysis[31] of the IR data was performed to check for any possible distribution into n different Pt particle species ($n = 1$ to 5). The decomposition result obtained with $n = 2$ appears as the most appropriate and explained up to 98% of the variations in the spectra on such WI samples.[31] The two separate contributions are identified in the spectra (Figure 2a) for WI_{fresh}, as shown by the area normalized reference spectra (Figure 2b). The relative contributions of the absorbance at low and high wavenumbers vary with increasing doses of CO introduced. This proportion is expressed by the respective concentration profiles (Figure 2c).

The two reference spectra obtained after decomposition (Figure 2b) validate the previous suggestion about the main presence of two populations of Pt nanoparticles. The shape of the two reference spectra gives clues about the size and shape

[*] Dr. M. Rivallan, Dr. E. Seguin, Dr. S. Thomas, Dr. F. Thibault-Starzyk
Laboratoire Catalyse et Spectrochimie, ENSICAEN, Université de Caen, CNRS, 6 Bd Maréchal Juin, 14050 Caen (France)
Fax: (+33) 2-1452-822
E-mail: fts@ensicaen.fr

Dr. M. Lepage
Advanced Technology Division, Toyota Motor Europe NV/SA
Hoge Wei 33, 1930 Zaventem (The Netherlands)

N. Takagi
Power Train Material Engineering Division
Toyota Motor Corporation
1, Toyota-cho, Toyota, Aichi, 471-8572 (Japan)

Dr. H. Hirata
Advanced Material Engineering Division, Toyota Motor Corporation
1200, Mishuku, Susono, Shizuoka, 410-1193 (Japan)

[**] We would like to thank Toyota Motor Europe for financing this research project through the Open Call process. Dr. N. Takahashi, Dr. H. Shinjoh, and Dr. Y. Nagai from Toyota Central R&D Laboratory as well as Prof. S. Matsumoto and M. Miura from Toyota Motor Corporation are warmly thanked for their fruitful discussions. We also acknowledge Dr. Philippe Bazin and Dr. Francis Cruege for help in the development of the PJAS instrumentation and Dr. Chantal Gunther for her skilful assistance in electronics for the data acquisition.

Supporting information for this article is available on the WWW under http://dx.doi.org/10.1002/anie.200905181.

Table 1: BET, CO chemisorption, and TEM measurements on Pt/ZSM-5 catalysts.

Pt/ZSM-5 samples			Textural properties			CO chemisorption		TEM	
Pt loading method[a]	Si/Al	Ageing conditions	S_{BET} [$m^2 g^{-1}$]	Pore volume [$m^3 g^{-1}$]	Micropore volume [$m^3 g^{-1}$]	Dispersion [%]	r[b]	d_{big} [nm]	d_{small} [nm]
WI_{fresh}	28	fresh	331	0.24	0.17	3.9	1.6	6.0	2.5
WI_{CO}	28	CO, 1073 K	338	0.25	0.16	3.4	2.1	12.0	2.5
WI_{N2}	28	N_2, 1073 K	337	0.20	0.16	2.9	2.5	12.0	2.5
WI_{air}	28	air, 1073 K	331	0.21	0.15	1.4	1.6	20.0	5.0
CI	50	fresh	389	0.29	0.18	29.4	–	2.0	
IE	50	fresh	373	0.28	0.17	16.4	–	5.0[c]	

[a] WI = wet impregnation; CI = colloid impregnation; IE = ion exchange. [b] Platinum surface ratio between pores and external surface. [c] Cylindrical shape with $l > d$.

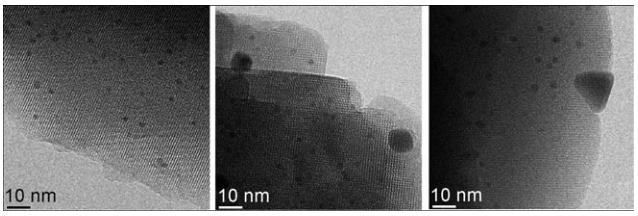

Figure 1. TEM images of WI_{fresh}, WI_{N2}, and WI_{air} samples (from left to right).

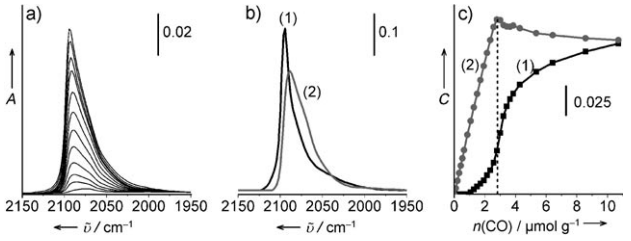

Figure 2. a) Difference IR spectra after CO additions on WI_{fresh} and b) corresponding MCR decomposition into two reference spectra. c) Concentration profiles. *C* is dimensionless and expressed as the relative contribution of the two reference spectra in (b) to the spectra displayed in (a) (the dotted line corresponds to saturation).

of the particles. The reference spectrum (1) is essentially centered on the 2095 cm^{-1} IR band; it corresponds to large particles for which CO is mainly adsorbed on Pt^0 planes (highly coordinated surface platinum atoms). The reference spectrum (2) is red-shifted and peaks at 2085 cm^{-1} with a broad shoulder at lower frequencies. It can be ascribed to smaller Pt particles for which CO adsorbs abundantly on less coordinated Pt atoms (at edges and corners) in the 2080–2050 cm^{-1} wavenumber range.[6,28] The spectra corresponding to these small particles (2) grow faster in intensity during the first CO doses (Figure 2c), indicating a preferential adsorption on small particles. Figure 3 reports the reference spectra from the chemometric analysis for the fresh and CO, N_2, or air aged samples. The chemometric analysis done on CI and IE samples only gives relevant decompositions with $n = 1$, indicating a homogeneous distribution of Pt particles in only one population on these samples.

The clear blue-shift (up to $\Delta\tilde{\nu}_{CO} \approx 5\ cm^{-1}$) observed for the second reference spectrum after ageing indicates agglomeration of small Pt particles (Figure 3b). Figure 3c shows the

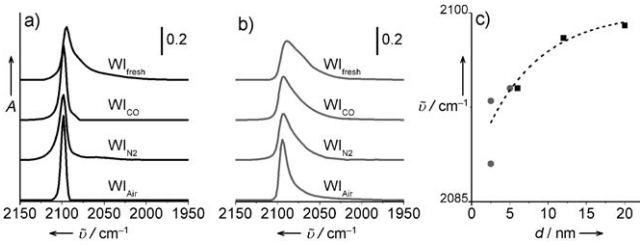

Figure 3. The 2150–1950 cm^{-1} range of the normalized reference spectrum of CO chemisorbed on a) large and b) small Pt particles of WI samples, as computed with the MCR-ALS method. Note that the CO and N_2 treatments lead to similar Pt particle distributions. c) Relationship between the frequency of the IR band (ν_{CO}) and particle size.

relationship between the frequency of the IR band (ν_{CO}) with particle size, determined as explained for Figure 4 (and detailed in Ref. [31]). The phenomenon is more pronounced on the mid-aged sample, and even more in the air aged sample—the broad shoulder corresponding to low coordinated Pt atoms is not visible anymore. The first reference spectrum (Figure 3a) corresponds to larger agglomerates; it is also blue-shifted and sharpened upon ageing, which also indicates sintering.

The Pt particle size was evaluated for both populations (assuming minimal Pt migration between the two distinct locations), considering a reference sample with known particle size (from TEM). The WI_{air} sample was preferred as starting point to calculate the sizes of large and small

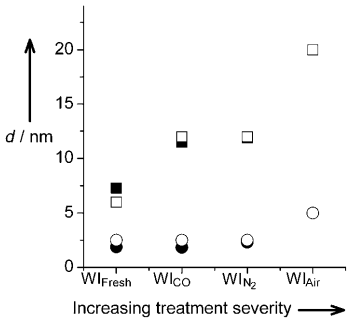

Figure 4. Determination of Pt particle sizes for the large (squares) and small particles (circles) from chemometric calculations (solid symbols; with WI_{air} as reference) and after TEM observations (empty symbols).

particles ("d_L" and "d_S") of the three other samples as difference between the two populations are the most obvious. These results agree very well with the TEM observations (Figure 4). It is also possible to have direct access to the ratio of large versus small Pt particles. It appears that 70% of Pt is present as large particles (above 6 nm) for WI, thus explaining the initial low dispersion on fresh sample.

The 2D PJAS-IR technique is capable of locating adsorption sites by Fourier analysis of the evolution of the IR spectrum after a sudden change in the pressure of adsorbed species over a porous material.[29] The pressure jump of adsorbed CO was studied on some of the samples to investigate the Pt location. In the corresponding 2D maps (Figure 5), two different frequency regions appear for the IR bands of both CO gas (2140–2120 cm^{-1}; high wavenumbers, HW) and adsorbed CO on Pt (2100–2000 cm^{-1}; low wavenumbers, LW). One resonance is at high frequency (HF) at 130 Hz or 250 Hz, depending on the Si/Al ratio and textural properties (Table 1), and a second one is at low frequency (LF; below 50 Hz). The IE sample, which should mainly contain platinum in the pores, exhibits essentially one single response at 130 Hz, that is, higher than on CI sample (<50 Hz). This latter frequency should be addressed to the CO adsorption–desorption oscillation process occurring on the external surface, as the colloid precursor is too large to penetrate into the zeolite pores. The difference in frequency observed between the two resonances can be explained in terms of the mean free path, which is shorter in the pores than on the outer surface. The WI_{CO} sample leads to oscillations at HF and LF, which confirms the presence of both Pt particles in the mesopores and on the external surface. Furthermore, the HF signal appears below 2070 cm^{-1} whereas the LF signal appears at higher wavenumbers.

It can be concluded that Pt particles located in the mesopores (with a resonant response at HF) are the smallest (CO peak centered at LW), whereas larger Pt particles (CO peak centered at LW) are observed on the outer surface of the zeolite (with a LF resonant response).

The Pt sintering mechanism is supposed to be mostly related to particle migration and coalescence after such thermal ageing treatments (1073 K),[32] so that Pt migration from the pores to the external surface must be clearly limited. Figure 6 depicts the sintering of the Pt particles occurring in two distinct and separated systems: inside the pores for small particles and on the external surface for large particles. When sintering occurs in the mesopores, the particle size is especially depending on the mean pore diameter, whereas on the external surface the particles may greatly agglomerate.

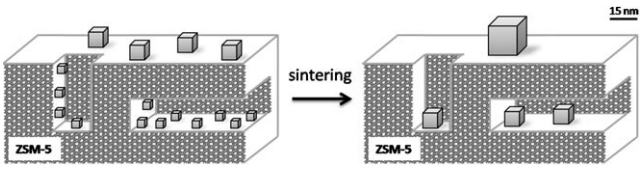

Figure 6. Sintering mechanism on Pt/ZSM-5 catalysts on the external surface and in the mesopores.

IR study of CO chemisorption on Pt/ZSM-5 catalysts has clearly confirmed the TEM observation of global sintering occurring after ageing under CO, N_2, and air. Chemometrics

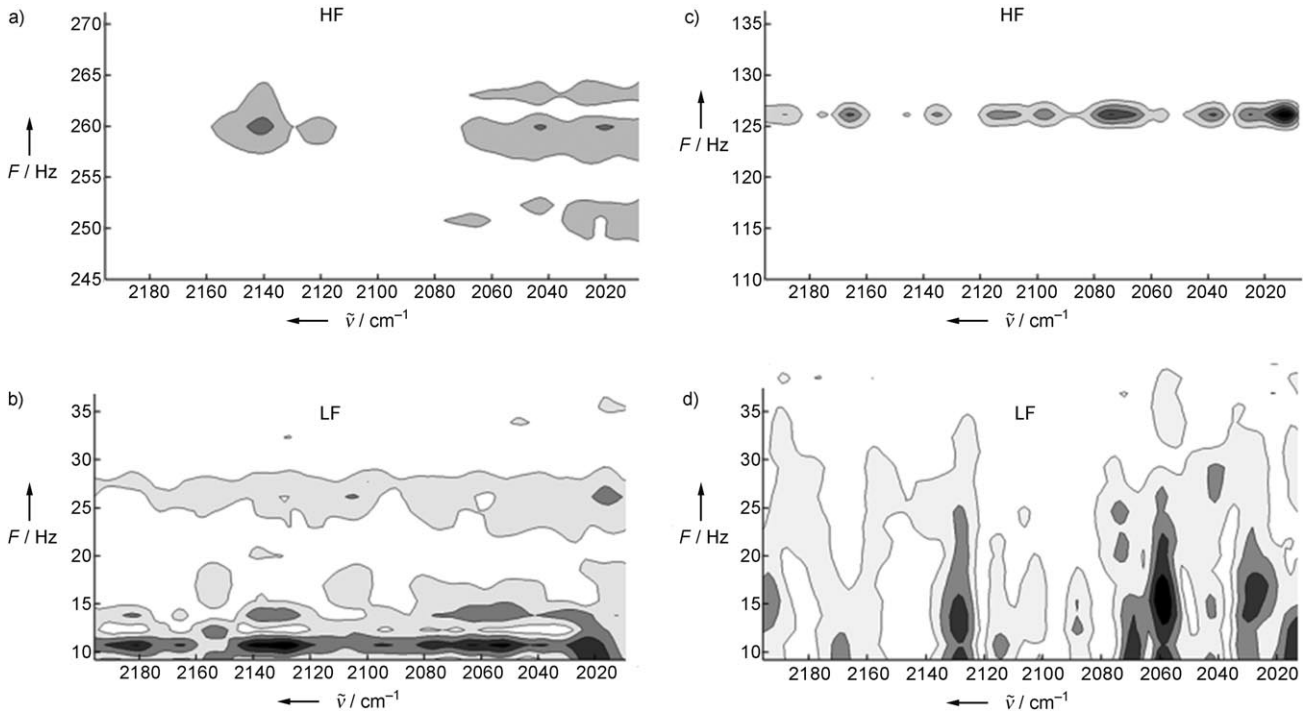

Figure 5. 2D PJAS-IR maps (at 573 K) of CO adsorbed on Pt/ZSM-5: WI_{CO} at a) HF and b) LF; c) IE at HF; and d) CI at LF. (IE at LF and CI at HF do not lead to any signal.)[31]

evidenced and quantified two separate populations of Pt nanoparticles differing in size. 2D PJAS-IR measurements showed the presence of Pt species in two different locations. Two relaxation frequencies range were found for one series of samples attributable to Pt particles located in the pores and on the external surface of the zeolite support. Some other samples only displayed one frequency because of the unique location for Pt particles: either in the pores or on the surface. After combination of the three techniques (chemisorption, chemometrics, and 2D PJAS-IR), two separate sintering mechanisms were observed on the ZSM-5 support:

- a limited sintering occurring in the mesopores, where the Pt particles size is restricted to the mean mesopore diameter (ca. 5 nm); and
- a much more pronounced sintering on the external surface, where severe thermal treatments lead to strong Pt particles agglomeration (ca. 20 nm) with no control by the support porosity.

The zeolite porosity, the corresponding Pt location (surface and porosity) after impregnation and thermal treatment, and possible migration are the key parameters that directly act on the severity of the deactivation mechanism. The benefit of the present spectroscopic techniques must now be linked to catalytic activity in CO oxidation (for example) to determine the optimum catalyst.

Experimental Section

Three Pt/ZSM-5 samples (2 wt.%) were prepared from colloid and wet impregnations (CI and WI) or after ion exchange (IE). The CI process was done from a solution of $H_2[PtCl_6]$ with polyvinylpyrrolidone as protective polymer and ethanol as reductant.[33] For WI, ZSM-5 powder was dispersed in distilled water and then added over the period of 1 h to a Pt nitrates solution (under stirring) and then heated to 363 K. Afterwards, the powder was dried in air at 393 K for 24 h and calcined in air at 723 K for 2 h. For IE, the ZSM-5 powder was dispersed in deionized water and stirred with a solution of $[Pt(NH_2)_4(OH)_2]$ for 2 h. After filtration and washing with deionized water, the Pt/ZSM-5 powder was finally dried and calcined. For the whole set of "ageing procedures", the sample (15 g) was first heated in a 25 mL cell from room temperature to 1073 K at 20 K min^{-1} under a flow of 5 L min^{-1} of dry N_2. The atmosphere was then switched to the desired ageing gas for 5 h at steady temperature and flow rate. At the end of the ageing treatment, the flowing gas was switched to dry N_2 and the samples were cooled to room temperature at 20 K min^{-1}.[31]

CO chemisorption experiments were measured with a static experimental FTIR setup.[31] Subsequent chemometric calculations were performed by using the multivariate curve resolution/alternating least squares (MCR-ALS) method.[31]

Two-dimensional pressure-jump IR spectroscopy of the adsorbed species (2D PJAS-IR) was performed on a Bruker IFS 66 FTIR instrument equipped with a cryogenic MCT detector and running at 8 cm^{-1} resolution.[31] The sample was in the form of self-supporting pellets suitable for measurements in transmission mode. A mixture of CO/He (1:10; 33 Torr) was introduced at room temperature, and then the sample was heated to 573 K. Afterwards, the 2D PJAS-IR experiment was performed on Pt/ZSM-5 with five co-additions and the IR spectra were recorded in step–scan mode with a time resolution of 1 ms.[34–36] This technique allows fast spectra acquisition in the first key steps of the process under study.[37]

Received: September 16, 2009
Revised: November 3, 2009
Published online: December 16, 2009

Keywords: chemometry · heterogeneous catalysis · IR spectroscopy · sintering · zeolites

[1] S. I. Matsumoto, *Catal. Today* **2004**, *90*, 183.
[2] H. S. Gandhi, G. W. Graham, R. W. McCabe, *J. Catal.* **2003**, *216*, 433.
[3] D. E. Webster, *Top. Catal.* **2001**, *16*, 33.
[4] B. M. Weckhuysen, *Angew. Chem.* **2009**, *121*, 5008; *Angew. Chem. Int. Ed.* **2009**, *48*, 4910.
[5] M. B. J. Roeffaers, G. De Cremer, H. Uji-i, B. Muls, B. F. Sels, P. A. Jacobs, F. C. De Schryver, D. E. De Vos, J. Hofkens, *Proc. Natl. Acad. Sci. USA* **2007**, *104*, 12603.
[6] P. Bazin, O. Saur, J. C. Lavalley, M. Daturi, G. Blanchard, *Phys. Chem. Chem. Phys.* **2005**, *7*, 187.
[7] K. Chakarova, M. Mihaylov, K. Hadjiivanov, *Catal. Commun.* **2005**, *6*, 466.
[8] K. Chakarova, M. Mihaylov, K. Hadjiivanov, *Microporous Mesoporous Mater.* **2005**, *81*, 305.
[9] P. Kubanek, H. W. Schmidt, B. Spliethoff, F. Schüth, *Microporous Mesoporous Mater.* **2005**, *77*, 89.
[10] A. G. Pelmenschikov, R. A. Vansanten, J. Janchen, E. Meijer, *J. Phys. Chem.* **1993**, *97*, 11071.
[11] A. Y. Stakheev, E. S. Shpiro, O. P. Tkachenko, N. I. Jaeger, G. Schulz-Ekloff, *J. Catal.* **1997**, *169*, 382.
[12] V. Alfredsson, O. Terasaki, Z. Blum, J. O. Bovin, G. Karlsson, *Zeolites* **1995**, *15*, 111.
[13] J. de Graaf, A. J. van Dillen, K. P. de Jong, D. C. Koningsberger, *J. Catal.* **2001**, *203*, 307.
[14] O. A. Anunziata, A. R. Beltramone, Z. Juric, L. B. Pierella, F. G. Requejo, *Appl. Catal. A* **2004**, *264*, 93.
[15] S. Bernal, J. J. Calvino, M. A. Cauqui, J. M. Gatica, C. Larese, J. A. P. Omil, J. M. Pintado, *Catal. Today* **1999**, *50*, 175.
[16] R. Burch, S. Scire, *Appl. Catal. B* **1994**, *3*, 295.
[17] A. Fukuoka, N. Higashimoto, Y. Sakamoto, M. Sasaki, N. Sugimoto, S. Inagaki, Y. Fukushima, M. Ichikawa, *Catal. Today* **2001**, *66*, 23.
[18] A. Goguet, D. Schweich, J. P. Candy, *J. Catal.* **2003**, *220*, 280.
[19] F. J. Gracia, L. Bollmann, E. E. Wolf, J. T. Miller, A. J. Kropf, *J. Catal.* **2003**, *220*, 382.
[20] P. O. Graf, D. J. M. de Vlieger, B. L. Mojet, L. Lefferts, *J. Catal.* **2009**, *262*, 181.
[21] M. Lepage, T. Visser, A. M. J. van der Eerden, F. Soulimani, B. M. Weckhuysen, *Vib. Spectrosc.* **2008**, *48*, 92.
[22] R. López-Fonseca, J. I. Gutiérrez-Ortiz, M. A. Gutiérrez-Ortiz, J. R. González-Velasco, *Catal. Today* **2005**, *107–108*, 200.
[23] K. I. Pandya, S. M. Heald, J. A. Hriljac, L. Petrakis, J. Fraissard, *J. Phys. Chem.* **1996**, *100*, 5070.
[24] V. Perrichon, L. Retailleau, P. Bazin, M. Daturi, J. C. Lavalley, *Appl. Catal. A* **2004**, *260*, 1.
[25] T. Sato, K. Kunimatsu, H. Uchida, M. Watanabe, *Electrochim. Acta* **2007**, *53*, 1265.
[26] J. I. Villegas, D. Kubicka, H. Karhu, H. Österholm, N. Kumar, T. Salmi, D. Y. Murzin, *J. Mol. Catal. A* **2007**, *264*, 192.
[27] T. Visser, T. A. Nijhuis, A. M. J. van der Eerden, K. Jenken, Y. Y. Ji, W. Bras, S. Nikitenko, Y. Ikeda, M. Lepage, B. M. Weckhuysen, *J. Phys. Chem. B* **2005**, *109*, 3822.
[28] R. M. Rioux, J. D. Hoefelmeyer, M. Grass, H. Song, K. Niesz, P. D. Yang, G. A. Somorjai, *Langmuir* **2008**, *24*, 198.
[29] S. Chenevarin, F. Thibault-Starzyk, *Angew. Chem.* **2004**, *116*, 1175; *Angew. Chem. Int. Ed.* **2004**, *43*, 1155.
[30] F. Thibault-Starzyk, S. Chenevarin, C. Fernandez, *Stud. Surf. Sci. Catal.* **2004**, *154*, 1730.

[31] See the Supporting Information for details.
[32] A. K. Datye, Q. Xu, K. C. Kharas, J. M. McCarty, *Catal. Today* **2006**, *111*, 59.
[33] N. Toshima, M. Harada, Y. Yamazaki, K. Asakura, *J. Phys. Chem.* **1992**, *96*, 9927.
[34] W. Barowy, H. Saki, *Infrared Phys.* **1984**, *24*, 251.
[35] T. J. Johnson, A. Simon, J. M. Weil, G. W. Harris, *Appl. Spectrosc.* **1993**, *47*, 1376.
[36] H. Sakai, R. E. Murphy, *Appl. Opt.* **1978**, *17*, 1342.
[37] F. Thibault-Starzyk, E. Seguin, S. Thomas, M. Daturi, H. Arnolds, D. A. King, *Science* **2009**, *324*, 1048.

